SPANDIDOS PUBLICATIONS

INTERNATIONAL JOURNAL OF ONCOLOGY 64: 29, 2024

UBDP1 pseudogene and UBD network competitively bind miR-6072 to promote glioma progression

FAN HONG[1,2*], ZHENYU GONG[3*], CHAO CHEN[2*], TIANZHEN HUA[2], QILIN HUANG[2], YU'E LIU[4], PEIPEI MA[2], XU ZHANG[2], HONGXIANG WANG[2] and JUXIANG CHEN[2]

[1]Department of Neurosurgery, Second Affiliated Hospital of Anhui Medical University, Anhui Medical University, Hefei, Anhui 230601; [2]Department of Neurosurgery, Changhai Hospital, Naval Medical University, Shanghai 200433, P.R. China; [3]Department of Neurosurgery, Klinikum rechts der Isar, Technical University of Munich, D-81675 Munich, Germany; [4]Tongji University Cancer Center, Shanghai Tenth People's Hospital of Tongji University, School of Medicine, Tongji University, Shanghai 200092, P.R. China

Received February 22, 2023; Accepted December 20, 2023

DOI: 10.3892/ijo.2024.5617

Abstract. Increasing evidence suggests that pseudogenes play crucial roles in various cancers, yet their functions and regulatory mechanisms in glioma pathogenesis remain enigmatic. In the present study, a novel pseudogene was identified, UBDP1, which is significantly upregulated in glioblastoma and positively correlated with the expression of its parent gene, UBD. Additionally, high levels of these paired genes are linked with a poor prognosis for patients. In the present study, clinical samples were collected followed by various analyses including microarray for long non-coding RNAs, reverse transcription-quantitative PCR, fluorescence *in situ* hybridization and western blotting. Cell lines were authenticated and cultured then subjected to various assays for proliferation, migration, and invasion to investigate the molecular mechanisms. Bioinformatic tools identified miRNA targets, and luciferase reporter assays validated these interactions. A tumor xenograft model in mice was used for *in vivo* studies. *In vitro* and *in vivo* studies have demonstrated that UBDP1, localized in the cytoplasm, functions as a tumor-promoting factor influencing cell proliferation, migration, invasion and tumor growth. Mechanistic investigations have indicated that UBDP1 exerts its oncogenic effects by decoying miR-6072 from UBD mRNA, thus forming a competitive endogenous RNA network, which results in the enhanced oncogenic activity of UBD. The present findings offered new insights into the role of pseudogenes in glioma progression, suggesting that targeting the UBDP1/miR-6072/UBD network may serve as a potential therapeutic strategy for glioma patients.

Correspondence to: Professor Hongxiang Wang or Professor Juxiang Chen, Department of Neurosurgery, Changhai Hospital, Naval Medical University, 168 Changhai Road, Shanghai 200433, P.R. China
E-mail: wanghongxiang27@smmu.edu.cn
E-mail: juxiangchen@smmu.edu.cn

[*]Contributed equally

Key words: glioblastoma, pseudogene, UBDP1, UBD, microRNA-6072

Introduction

Glioblastoma (GBM) is the most prevalent malignant primary brain tumor in adults, constituting 54% of all glioma cases (1). Despite standard treatment involving surgery followed by concurrent chemoradiotherapy and adjuvant chemotherapy, the curative effect remains limited, with a median patient survival time of only ~15 months (2). Consequently, there is a pressing need to explore the biological nature of GBM, decipher the signaling pathways underpinning tumor progression, and develop therapeutic strategies targeting driver factors to improve disease management and patient lifespan.

Pseudogenes, a distinct class of long non-coding RNAs (lncRNAs), have sequences that are dysfunctional copies of protein-coding genes. Yet, burgeoning evidence suggests their involvement in various biological processes, and their role in significant functions (3). Generally, pseudogenes can be transcribed into antisense RNA to meddle with coding genes or act as competitive endogenous RNA by binding to microRNAs (miRNAs) (4). Numerous studies have indicated that pseudogene dysregulation may contribute to disease development, including tumors. For instance, the pseudogene PTENP1 can exert a growth-suppressive function by regulating cellular levels of PTEN through competitive miRNA binding, but its gene locus is selectively lost in human cancer (5). A network made up of numerous miRNAs and several pseudogenes, all originating from a single parent gene, can be controlled through various mechanisms. Disruption or dysregulation of this intricate network can lead to the onset and progression of cancer, such as the case with an FTH1 pseudogene observed in prostate cancer (6). Genomic gains and aberrant expression of BRAFP1, which serves as a ceRNA sponge for miRNAs

targeting BRAF, can elicit its oncogenic activity and induce lymphoma (7). The enhancement of mitochondrial fission is facilitated by RACGAP1P via a mechanism that depends on its competitive interaction with miR-345-5p, counteracting its parent gene, RACGAP1. This process culminates in the activation of dynamin-related protein 1 (Drp1), and advances the invasion and metastasis of breast cancer (8). Despite previous revelations about the prognostic value of two pseudogene signatures in glioma cohorts, understanding of pseudogene expression patterns, functions and regulatory mechanisms in glioma remains limited (9,10). Only a handful of tumor-promoting pseudogenes have been identified in glioma: Hypoxia-induced PDIA3P1, which facilitates mesenchymal transition through the PDIA3P1/miR-124-3p/RELA axis; LGMNP1, which elevates LGMN expression by sponging miR-495-3p; and ANXA2P2, which competes with miR-9 against LDHA to modulate aerobic glycolysis progression and tumor cell proliferation (11-13).

Pseudogene UBDP1, residing on chromosome 6p22.1 and spanning 271 bp, exhibits a high degree of sequence homology with its coding gene UBD, also known as FAT10. This ubiquitin-like regulatory protein with a proteasome degradation signal (14) is overexpressed in a variety of solid tumors, including those of the breast, stomach, colon, liver and pancreas. It also promotes the invasion and metastasis of hepatocellular carcinoma (15), the metastasis of osteosarcoma (16), breast cancer invasion (17) and the chemotherapy resistance of non-small cell lung cancer (18). Its overexpression and oncogenic activity have been identified in glioma as well (19,20). Yet, the interaction and role of the UBDP1-UBD binary system in glioma progression remain largely unexplored.

The present study identified a novel pseudogene, UBDP1, which is upregulated in GBM and associated with a poor patient prognosis. Further *in vitro* and *in vivo* investigations demonstrated that both UBDP1 and UBD foster GBM proliferation, migration and invasion. UBDP1 serves as an endogenous sponge for miR-6072, obstructing its interaction with UBD, subsequently enhancing UBD's oncogenic capabilities and promoting tumor advancement. These findings illustrated the intricate pseudogene regulatory network within GBM and highlight a potential therapeutic target.

Materials and methods

Clinical samples. Tumor specimens were obtained from patients who were initially diagnosed with GBM and underwent their first surgical procedure between December 2016 and May 2020 at Shanghai Changzheng Hospital, Naval Medical University (Shanghai, China). The median age of patients was 49 (range, 34-65), comprising 15 men and 15 women. Normal brain tissues were obtained from craniocerebral trauma patients who received intracranial decompression therapy between January 2018 and May 2020 at the aforementioned hospital. The median age of patients was 41 years (range, 29-57). The present study was approved (approval no. CZEC2018-032) by the Independent Ethics Committee of Shanghai Changzheng Hospital (Shanghai, China). Written informed consent was obtained from all patients or their legal guardians indicating their understanding of the risks and benefits.

Microarray analysis. lncRNA microarray data were obtained from the authors' previous study (GEO dataset: GSE51146) (21). Differentially expressed lncRNAs were identified by using Volcano Plot filtering. The threshold of upregulated and downregulated lncRNAs was $P<0.05$ and a fold change >2.

Cell lines, authentication and culture conditions. Human cell lines U87MG (RRID: CVCL_0022), U251MG (RRID: CVCL_0021) and 293T (DSMZ no. ACC 635) were purchased from the Cell Bank at the Chinese Academy of Sciences (Shanghai, China). In order to authenticate these cell lines, STR profiling was conducted in the year 2020; the identities of these cell lines were confirmed and authenticated. The U87 cell line used in the present study is most probably an ATCC-originating version of the U87 MG cell line. All these cells were cultured in Dulbecco's modified Eagle's medium (DMEM) supplemented with 10% FBS (both from Hyclone; Cytiva) and 5% CO_2 at 37˚C.

Reverse transcription-quantitative PCR (RT-qPCR). Total RNA was extracted from tissues and cells using TRIzol reagent (Wuhan Servicebio Technology Co., Ltd.). RNA was reverse transcribed to cDNA using RevertAid First Strand cDNA Synthesis kit (Thermo Fisher Scientific, Inc.) according to the manufacturer's protocol. qPCR was performed using FastStart Universal SYBR Green Master (Roche Diagnostics) on the RT-PCR system (Applied Biosystems; Thermo Fisher Scientific, Inc.). The thermocycling conditions were as follows: The procedure involved 40 cycles, which consisted of denaturation at 98˚C for 10 sec, annealing at 58˚C for 25 sec and extension at 68˚C for 30 sec. GADPH was marked as an internal control. The primers used were as follows: GAPDH forward, 5'-GGAAGCTTGTCATCAATGGAAATC-3' and reverse, 5'-TGATGACCCTTTTGGCTCCC-3'; UBD forward, 5'-CAATGCTTCCTGCCTCTGTGT-3' and reverse, 5'-GGGTAAGGTGGATGGTCTTCTCT-3'; and UBDP1 forward, 5'-TGGCTGCTAAAATGGAGTGAAGA-3' and reverse, 5'-AGGTGAGGTGGATGGTCTTCTT-3'. The expression levels were determined using the $2^{-\Delta\Delta Cq}$ method (22).

Fluorescence in situ hybridization (FISH). The cells were fixed in 4% paraformaldehyde for 15 min at room temperature, washed with PBS, treated with pepsin (1% in 10 mM HCl), and dehydrated with 70, 85 and 100% ethanol. The cells were then air-dried and incubated in a hybridization buffer containing the FISH probe for 5 min at 73˚C in a water bath. The hybridization was performed for 12 h at 37˚C. After washing and dehydrating the cell slides, they were counterstained with DAPI (2.5 μg/ml). The RNA FISH probe for UBDP1 was designed and synthesized by Shanghai GenePharma Co., Ltd., and its sequence was 5'-FAM-CCTACCTTCTTCACTCCATTTTAGCAGCCA-FAM-3'.

Plasmid construction. The gene sequences and target sequences of UBD and UBDP1 were constructed into the GV657/GV248 vector plasmid (Shanghai GeneChem Co., Ltd.) by PCR amplification and double enzyme digestion (restriction enzymes, New England BioLabs, Inc.). Thus, GV657/UBD-Overexpression, GV657/UBDP1-Overexpression, GV248/UBD-Knockdown and GV248/UBDP1-Knockdown plasmids were obtained.

GV657/GV248 vector plasmids (Shanghai GeneChem Co., Ltd.) were used as negative control (NC). The sequences of PCR amplification primers were as follows: UBD overexpression forward, 5'-CGGAATTCATGGCTCCCAATGCTTCCT-3' and reverse, 5'-CGGGATCCTCACCCTCCAATACAATAACATGCCA-3'; UBD knockdown forward, 5'-CCGGCGAGACTAAGACGGGTATAATCTCGAGATTATACCCGTCTTAGTCTCGTTTTTG-3' and reverse, 5'-AATTCAAAAACGAGACTAAGACGGGTATAATCTCGAGATTATACCCGTCTTAGTCTCG-3'; UBDP1 overexpression forward, 5'-CGGAATTCGTTGGTGATACCTACTTTCACTGAG-3' and reverse, 5'-CGGGATCCGCATCTCTCTACCCCTGGG-3'; and UBDP1 knockdown forward, 5'-CCGGTCTGGTGGAAACATGTGATCAAGCTTCATCACATGTTTCCACCAGATTTTTG-3' and reverse, 5'-AATTCAAAAATCTGGTGGAAACATGTGATGAAGCTTGATCACATGTTTCCACCAGA-3'.

The gene sequences and target sequences of miR-6072 and miR-6818-3p were constructed into the GV251/GV249 vector plasmid (Shanghai GeneChem Co., Ltd.) by PCR amplification and double enzyme digestion (restriction enzymes, New England BioLabs, Inc.). Thus, the GV251/miR-6072-Overexpression, GV251/miR-6818-3p-Overexpression, GV249/miR-6072-Inhibition and GV249/miR-6818-3p-Inhibition plasmids were obtained. GV251/GV249 vector plasmids (Shanghai GeneChem Co., Ltd.) were used as NC. The sequences of PCR amplification primers were as follows: MiR-6072 overexpression forward, 5'-TGTGGAAAGGACGCGGGATCAGATGCACAGGACTGGGCAC-3' and reverse, 5'-CAGCGGTTTAAACTTAAGCTAAAAAATAAGAACTACTCTATG-3'; miR-6072 inhibition forward, 5'-GCTAAAAATCCTCATCACACTGCACCTTAGG-3' and reverse, 5'-ATCCCTAAGGTGCAGTGTGATGAGGATTTTT-3'; miR-6818-3p overexpression forward, 5'-ACGGGCCCTCTAGACTCGAGTGTTGGTTGTGTAAGATTTC-3' and reverse, 5'-TTAAACTTAAGCTTGGTACCTACTGACTGTACCAGATGC-3'; and miR-6818-3p inhibition forward, 5'-GCTAAAAATTGTCTCTTGTTCCTCACACAGG-3' and reverse, 5'-ATCCCTGTGTGAGGAACAAGAGACAATTTTT-3'. The vectors and DNA fragments were then connected using T4 ligase from New England BioLabs, Inc.

Cell transfection. U87 and U251 cell lines were cultured to a density of $2x10^5$ cells for transfection purposes. Transfection was performed using 50 pmol of either miRNA mimics or inhibitors. Lipofectamine® 3000 (Thermo Fisher Scientific, Inc.) was employed as the transfection reagent, and 5 μl was administered to each well of a 6-well plate, as per the manufacturer's instructions. To prepare the transfection mix, Lipofectamine® 3000 was first diluted in Opti-MEM Medium (Gibco; Thermo Fisher Scientific, Inc.) and thoroughly mixed. Separately, a master mix of the DNA was prepared by diluting the desired amount of DNA also in Opti-MEM Medium and mixing until being homogeneous. The diluted DNA was then combined with the previously diluted Lipofectamine® 3000, using a 1:1 ratio, to form a DNA-lipid complex. This complex was allowed to incubate for 20 min at room temperature (37˚C) to facilitate the formation of a stable DNA-lipid complex. Subsequently, the complex was administered to the cultured cells. Following transfection, the cells were incubated at 37˚C for a period of 48 h prior to conducting any subsequent experiments. For lentiviral transduction, the vectors (GL132/GV248; Shanghai GenePharma Co., Ltd.) were co-transfected with helper in the 2nd generation transfection system into 293T cells. The 293T cells were cultured in DMEM supplemented with 10% FBS at a temperature of 37˚C and a CO_2 concentration of 5%. Following a 48-h incubation period at 37˚C, the supernatant of the 293T cells were collected and the lentivirus was concentrated by subjecting to centrifugation at 25,000 x g for 2 h at 4˚C. The harvested lentiviral vectors were then introduced into the target GBM cells (U87/U251) for transduction. Subsequently, U87/U251 cell lines were plated into a 6-well plate and the cells were cultured until they reach 80% confluence. To generate stable cell lines, GBM cells were transduced with these lentiviral vectors in a milieu containing polybrene (Shanghai GenePharma Co., Ltd.) at a concentration of 5 μg/ml. Then, lentivirus was added and co-cultured with the cells at 37˚C for 24 h (Multiplicity of infection, 10). After that, the medium was replaced, and then culture continued in a 5% CO_2 and 37˚C incubator for another 48 h. Following a 72-h incubation period, cells underwent a selection process using 2 μg/ml of puromycin (Shanghai GeneChem Co., Ltd.), over a course of 3 days.

Western blot analysis. Cell lysates were prepared with RIPA buffer (Thermo Fisher Scientific, Inc.). The proteins were separated using 10% SDS-PAGE and then transferred to PVDF membranes (EMD Millipore), and a total of 25 μg protein were loaded per lane. After 2 h of blocking using 5% milk at room temperature, membranes were incubated overnight at 4˚C with different primary antibodies (FAT10 Rabbit mAb; 1:1,000; cat. no. 76194; Cell Signaling Technology, Inc.). The membranes were then incubated at room temperature for 1 h with secondary antibodies (Anti-rabbit IgG HRP-linked antibody; 1:10,000; cat. no. 7074; Cell Signaling Technology, Inc.; RRID: AB_2099233), and the bands were detected using a chemiluminescence imager (Syngene) and analyzed with Image Lab™ Software (version 5.1; Bio-Rad Laboratories, Inc.). GAPDH (1:1,000; cat. no. sc-47724; Santa Cruz Biotechnology, Inc.) served as the control.

Cell proliferation assay. The proliferation ability of the cells was tested using the Cell Counting Kit-8 assay (CCK-8; Shanghai Yeasen Biotechnology Co., Ltd.), according to the manufacturer's instructions. Cells were seeded in a 96-well plate at a density of 1,000-2,000 each and cultured at 37˚C. At the indicated time points (0, 24, 48, 72 and 96 h), 10 μl CCK-8 was added to the plate for 4 h. The optical density at 450 nm was measured consecutively using a microplate reader (Bio-Rad Laboratories, Inc.). Each experiment was performed thrice.

Cell migration and invasion assays. The migration assays were performed using the uncoated plates in Transwell chambers (8-μm diameter pores; Corning, Inc.), while Matrigel-coated plates were used for invasion assays at 37˚C for 1 h. The upper chambers contained $2x10^4$ cells/well in serum-free medium, while FBS with 10% serum was loaded into the lower chamber. After 24 h of incubation at 37˚C with 5% CO_2 in the humidified incubator, the cells were stained with 0.4% crystal

violet at room temperature for 10 min. The remaining cells in the upper chamber were removed with cotton swabs, while the migratory or invasive cells in the lower chamber were counted under a light microscope.

Bioinformatic analysis. The miRanda tool (http://www.microRNA.org/) was used to predict binding sites between miRNAs, UBD mRNA, and UBDP1, with Score and Energy thresholds of >140 and <-20, respectively. The screened miRNAs targeting UBD and UBDP1 were subsequently matched against databases, including miRWalk 3.0 (http://mirwalk.umm.uni-heidelberg.de/), miRDB (https://mirdb.org/), ENCORI (https://rnasysu.com/encori/), microRNA (https://mirbase.org/), Tarbase (http://diana.imis.athena-innovation.gr/DianaTools/index.php?r=tarbase/index) and miRNet (https://www.mirnet.ca/). Then, the miRNA(s) shared by the maximum number of databases and binding with maximum similarity to the UBD mRNA and UBDP1 sequences were identified.

Luciferase reporter assay. The dual luciferase reporter plasmids [GM-1013FL02 + UBDP1 mutant (MT)/wild-type (WT), GM-1013FL02 + UBD MT/WT] were designed and synthesized by Shanghai GenePharma Co., Ltd. Co-transfection was conducted with Lipofectamine® 3000 for 48 h. The activities of the firefly and *Renilla* luciferases were analyzed using a dual luciferase assay kit (cat. no. E1910; Promega Corporation), according to the manufacturer's instructions. The assay was conducted independently in triplicate.

Tumor xenograft model. Nude female BALB/cA (RRID: MGI:2160349) mice (age, 4 weeks-old) were purchased from the Shanghai Jihui Laboratory Animal Care Co., Ltd. The nude mice were kept in separate ventilated cages within a controlled environment that was free from pathogens, and they were provided with free access to food and water. The mice were subjected to a 12/12-h light/dark cycle, with the temperature maintained between 20-25˚C and humidity levels ranging from 50-80%. At the time of tumor cell injection, each mouse weighed ~18±1.75 g and was 6 weeks-old. They were divided into three groups (n=9 in each group). The mice were subjected to anesthesia through intraperitoneal injection of ketamine (100 mg/kg) and xylazine (20 mg/kg). Subsequently, they were secured in a stereotaxic frame (Kopf Instruments) and placed on a heating pad to ensure temperature maintenance. After careful sterilization, 2 μl PBS containing $1x10^7$ U87 cells were injected using a Hamilton micro-syringe in the mice's parietooccipital median region with the depth 2-3 mm, the whole injection period lasting for 2 min. After injection, the health and behavior of every nude mouse was monitored on a daily basis. The tumor burden in the mice began to adversely affect their quality of life, causing severe difficulties in fundamental activities such as drinking, eating and moving, thereby severely diminishing their comfort. Consequently, to minimize any further distress, all mice were compassionately euthanized using an intraperitoneal injection of pentobarbital (150 mg/kg). This was followed by a secondary verification of euthanasia, employing cervical dislocation to confirm the cessation of life. In total, 60 days after implantation, all mice were euthanized by intraperitoneal injection of pentobarbital and cervical dislocation. Cardiac arrest was then employed to confirm death by the examination of pulse palpation. The overall survival time from tumor implantation to the death of mice was then recorded. Their whole brains were removed when the mice were euthanized and immediately processed for histological evaluation. In the present investigation, the maximum tumor diameter was found to be <2 cm, and the maximum tumor volume was <2,000 mm^3. All mice experiments were performed according to the Institutional Guidelines for the Care and Use of Laboratory Animals of the Naval Medical University and were approved by the Animal Care and Experimental Committee of Naval Medical University (approval no. CZEC2018-032; Hefei, China).

Immunohistochemistry (IHC). The IHC assay was performed as previously described (23). The primary antibody used was Ki-67 Rabbit mAb (1:100; cat. no. 9027; Cell Signaling Technology, Inc.). The tumor tissues sections (5.0-μm-thick) were stained with hematoxylin and eosin (cat. no. G1003; Wuhan Servicebio Technology Co., Ltd.) at room temperature for 5 and 7 min, respectively.

Statistical analysis. All statistical analyses were performed using GraphPad Prism 6.0 (Dotmatics) and SPSS (RRID:SCR_002865) 18.0 software (IBM Corp.). The unpaired Student's t-test was used to compare the two groups. A one-way ANOVA test followed by Turkey's post hoc test was performed to analyze data among multiple groups. Pearson correlation analysis was applied to determine the linear relationship between the expression of different genes. The survival curves were calculated by the Kaplan-Meier method, and a log-rank test detected the difference. Univariate and multivariate survival analyses used the Cox hazard regression model; univariate analysis factors with P<0.1 were included in the multivariate analysis. Data were presented as the mean ± standard deviation (SD). P<0.05 was considered to indicate a statistically significant difference.

Results

UBDP1 and UBD are concomitantly highly expressed in GBM and correlate with a poor prognosis. From the authors' previous microarray data (GSE51146), differentially expressed lncRNAs in GBM were searched and eight upregulated and 29 downregulated pseudogenes were identified (Fig. 1A and Table SI). Among these dysregulated pseudogenes, UBDP1 was selected due to its significant expression shifts and unexplored functions in glioma (Fig. 1B). RT-qPCR was then utilized to assess UBDP1 expression in 30 GBM and 15 normal brain tissue samples, confirming a substantial upregulation of UBDP1 in GBM (Fig. 1C). Furthermore, analysis of the UBDP1 gene disclosed a pseudogene with 75% sequence similarity to UBD mRNA, which was also found to be significantly overexpressed in GBM (Fig. 1C), with its levels exhibiting a strong positive correlation with UBDP1 (Fig. 1D).

To elucidate the clinical significance of UBDP1 in GBM, clinical data from patients with GBM were collected, and patients were categorized based on their UBDP1 expression level (high and low) (Table I). When analyzed using the Kaplan-Meier curve and Cox hazard regression model, elevated

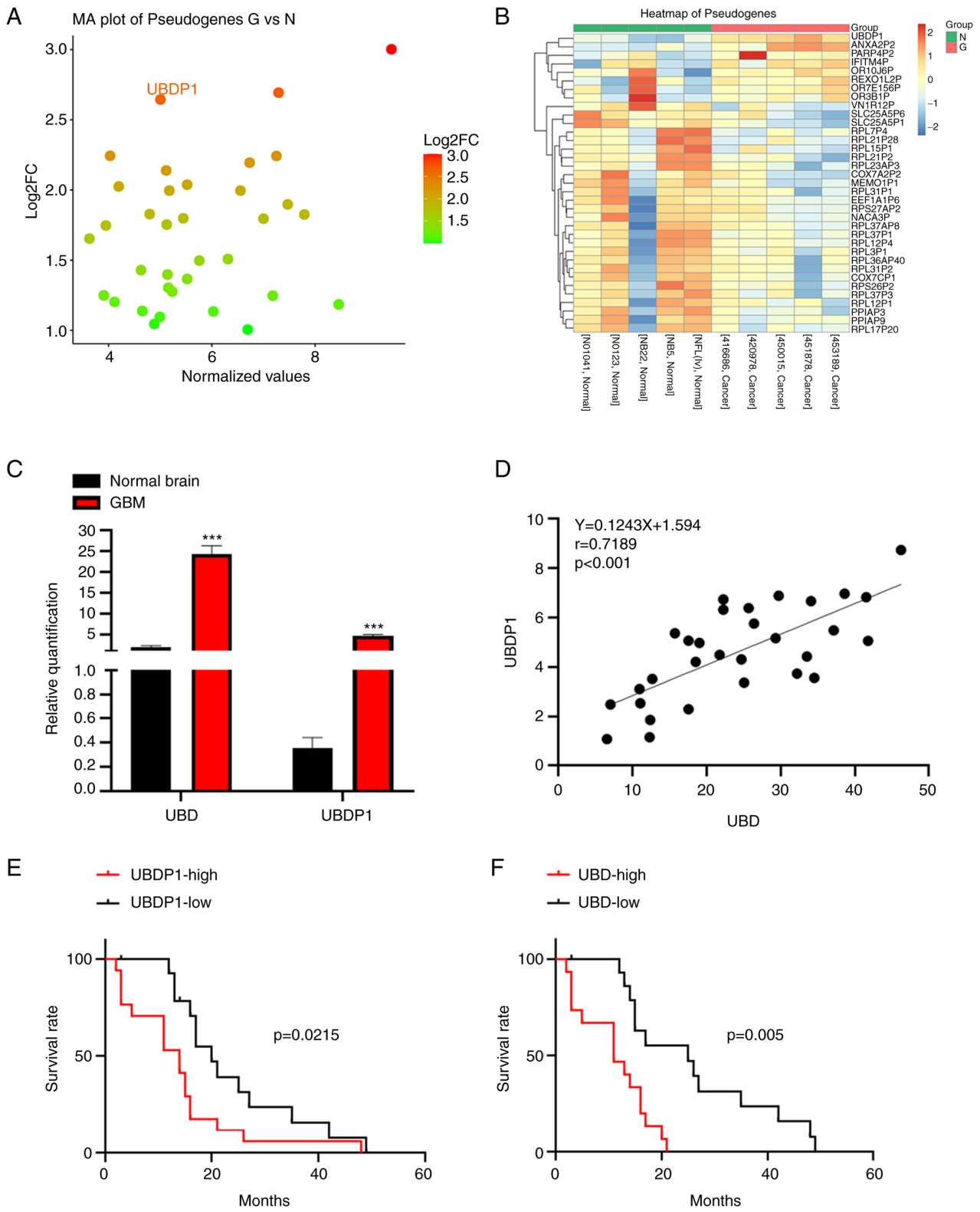

Figure 1. Pseudogene UBDP1 is upregulated and correlated with poor outcomes in GBM. (A) MA plot revealed dysregulated pseudogenes in GBM (G, glioblastoma; N, normal brain). (B) Heatmap demonstrated the differently expressed pseudogenes between GBM and normal brain. (C) Reverse transcription-quantitative PCR of 30 GBM samples and 15 normal brain tissues confirmed both the expression of UBDP1 and UBD upregulated in GBM compared with normal brain. (D) Pearson correlation analysis determined a strong relationship between UBDP1 and UBD expression of the 30 GBM samples. (E and F) Kaplan-Meier curve showed either high UBDP1 or high UBD expression associated with a short overall survival time of patients with GBM. n=3. ***P<0.001. GBM, glioblastoma.

UBDP1 expression significantly associated with shorter overall survival times (Fig. 1E) and presented as a potential independent risk factor (Tables II and SII). Consistently, high expression of UBD also associated with poor patient prognosis (Fig. 1F). These findings suggested that both UBDP1 and UBD could potentially drive GBM progression.

Table I. Clinicopathological characteristics and expression level of UBDP1 of 30 patients with glioblastoma.

Clinicopathological characteristics	Number of patients (n=30) (%)	Expression level of UBDP1	
		High (n=15)	Low (n=15)
Sex			
Male	15 (50)	5	10
Female	15 (50)	10	5
Age			
≤45	9 (30)	2	7
>45	21 (70)	13	8
Tumor size (cm)			
<4	15 (50)	11	4
≥4	15 (50)	4	11
Resection degree			
Total	26 (87)	11	15
Subtotal	4 (13)	4	0
Radio-chemotherapy			
Yes	23 (77)	11	12
No	7 (23)	4	3
IDH1 mutation			
Yes	2 (7)	0	2
No	28 (93)	15	13
UBD			
High	15 (50)	10	5
Low	15 (50)	5	10

UBDP1 and UBD promote proliferation, migration and invasion of glioma cells. To investigate the biological roles of UBDP1 and UBD in glioma, stable UBDP1- and UBD-overexpressing or knocking down cell lines [U87 and U251 (RRID: CVCL_1G29) cells] were established, validating their expressions using RT-qPCR and western blotting. Then, a CCK-8 assay was performed to determine the effect of UBDP1 and UBD on proliferation. Overexpression of UBDP1 and UBD increased the proliferation potential of glioma cells, whereas the knockdown of UBDP1 and UBD significantly impeded this capacity (Fig. 2A and B). Furthermore, Transwell and Matrigel assays were conducted to examine whether UBDP1 and UBD are involved in glioma migration and invasion. As indicated in Fig. 2C-F, upregulation of UBDP1 and UBD significantly accelerated glioma cell migration and invasion compared with the control group. By contrast, knockdown of UBDP1 and UBD decreased the number of migratory and invasive cells. These results demonstrated the tumor-promoting capacities of UBDP1 and UBD in glioma cells.

UBDP1 and UBD aggravate the malignancy of glioma in vivo. To determine the *in vivo* function of UBDP1 and UBD, U87 cells, either overexpressing UBDP1 or UBD or serving as a NC, were injected into the brains of nude mice. As expected, elevated levels of UBDP1 and UBD associated with reduced overall survival in xenograft mice relative to the NC group (Fig. 3B). To access tumor characteristics *in vivo*, additional five mice from each group were euthanized two weeks post-injection. H&E staining of xenograft sections revealed that mice bearing UBDP1 or UBD overexpressing U87 cells exhibited significantly enhanced tumor growth than mice in control group (Fig. 3A). Consistently, an IHC assay confirmed higher Ki-67 levels in xenograft samples overexpressing UBDP1 or UBD compared with the control group (Fig. 3C and D). Collectively, these results suggested that both UBDP1 and UBD contribute to the oncogenic progression of glioma.

Identification of the common miRNAs shared between UBD and UBDP1. The localization of UBDP1 in glioma cells was investigated using FISH and immunofluorescence assays. As demonstrated in Fig. 4A, UBDP1, similar to UBD, was predominantly found in the cytoplasm of U251 and U87 cells, suggesting its potential role as a miRNA sponge (Fig. 4A) (24,25). Several potential miRNA targets for UBDP1 were predicted using online databases (Table SIII) and two targets, miR-6072 and miR-6818-3p, were found to interact with both UBDP1 and UBD mRNA (Fig. 4B and C). To evaluate the influence of these miRNAs on UBD expression, 293T cells were transfected with miRNA mimics or inhibitors, and alterations in UBD protein levels were assessed via western blotting. Compared with the control, miR-6072 mimics were associated with a reduction in UBD levels, whereas miR-6072 inhibitors resulted in increased UBD expression. However, miR-6818-3p mimics presented conflicting results (Fig. 4D). Dual-luciferase reporter gene assays further confirmed that both UBDP1 and UBD were direct targets of miR-6072 (Fig. 4E and F). These findings suggested that miR-6072 plays a pivotal role in the competitive endogenous RNA network involving UBDP1 and UBD.

UBD is markedly activated through UBDP1 competitively binding to miR-6072 in glioma. To verify the hypothesis that UBDP1 functions as a competitive endogenous RNA, sequestering UBD from miRNA-6072 induced degradation, expression of UBD was analyzed in U87 and U251 cells transfected with either a miRNA-6072 mimic or an inhibitor. The results revealed that overexpression of miRNA-6072 significantly decreased the level of UBD in both glioma cells, whereas its inhibition increased the UBD expression (Fig. 5A). Additionally, the UBD expression was detected in U87 and U251 cells transfected with UBDP1 overexpression or knockdown vector and it was found that the level of UBD was markedly elevated in UBDP1-overexpressing glioma cells and notably decreased in UBDP1-knockdown cells (Fig. 5B). Moreover, co-transfection of UBDP1 and miR-6072 demonstrated that miR-6072 reversed the protein-level upregulation of UBD mediated by UBDP1 (Fig. 5C). UBDP1 was overexpressed in U87 and U251 glioma cells to determine the role of the UBD-miR-6072-UBDP1 network in glioma progression. Transfection with miR-6072 mimics counteracted the increased proliferative ability of UBDP1-overexpressing cells (Fig. 5D). Similarly, miR-6072 mimics diminished the enhanced invasion and migration capabilities prompted by UBDP1 (Fig. 5E and F). These

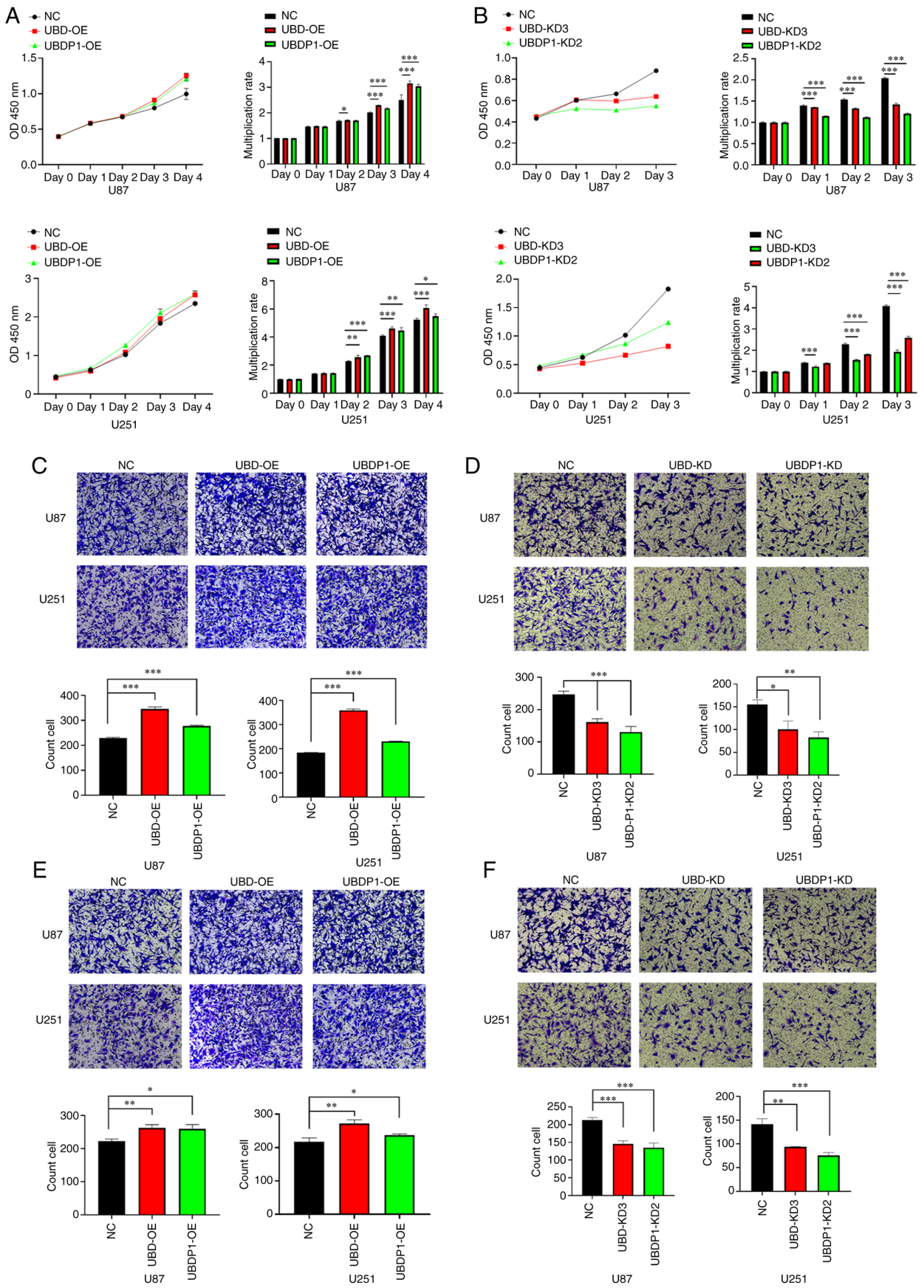

Figure 2. UBDP1 and UBD aggravate the malignancy of glioma cells. (A and B) Cell Counting Kit-8 assay revealed that overexpression of either UBDP1 or UBD could confer an enhanced proliferation ability on glioma cells, whereas knocking down UBDP1 or UBD inhibited cell proliferation. (C and D) Transwell assay (magnification, x100) displayed an increased number of migratory glioma cells in the UBDP1 or UBD overexpressing group compared with control groups but decreased glioma cells in the UBDP1 or UBD knocked down group. (E and F) Matrigel assay (magnification, x100) demonstrated stronger invasion of U87 and U251 with overexpression of UBDP1 or UBD but significantly less invasion ability of U87 and U251 with inhibition of UBDP1 or UBD when compared with that of NC. n=3. *P<0.05, **P<0.01, and ***P<0.001. KD, knockdown; NC, negative control; OE, overexpression.

Table II. Cox multivariate analysis of factors associated with overall survival of patients with glioblastoma.

Variable	Hazard ratio	95% confidence interval	P-value
UBDP1 (low vs. high)	4.114	1.484-11.405	0.007
Age (≤45 vs. >45)	6.649	2.060-21.459	0.002
Tumor size (<4 cm vs. ≥4 cm)	7.021	1.829-26.945	0.009
Resection degree (Total vs. Subtotal)			0.106
Radio-chemotherapy (Yes vs. No)	0.173	0.042-0.704	0.014
IDH1 mutation (Yes vs. No)			0.175

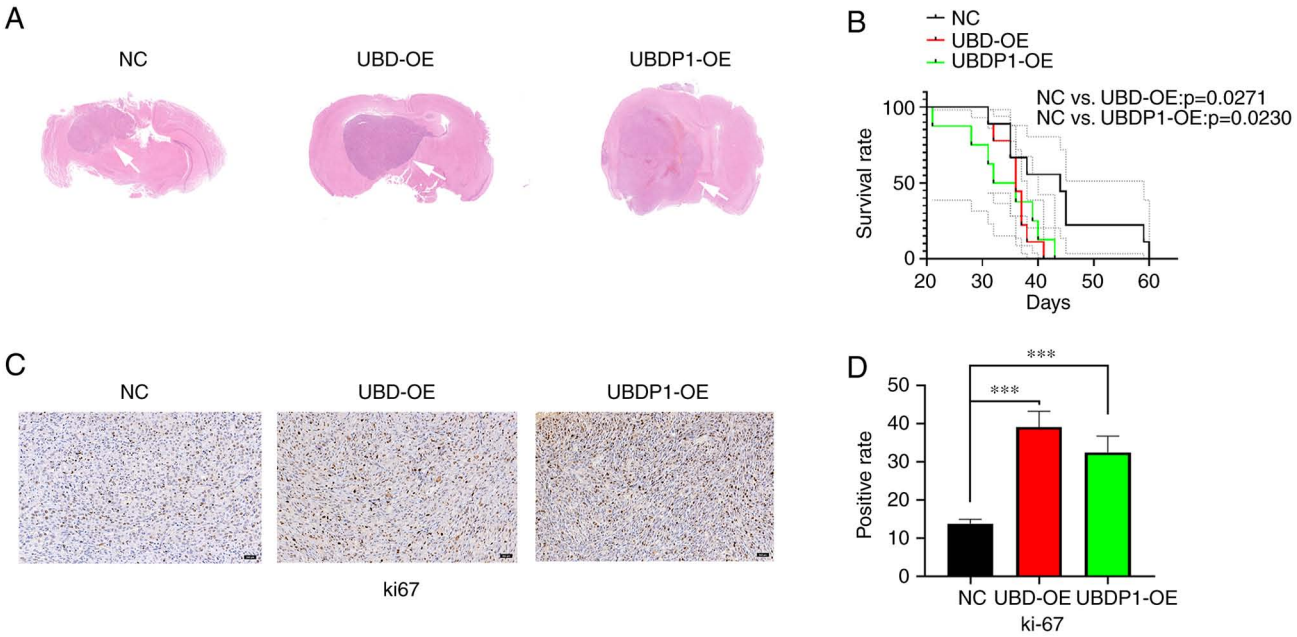

Figure 3. UBDP1 and UBD promote glioma growth *in vivo*. (A) H&E staining of xenograft sections demonstrated tumor sizes in different xenograft mice groups. (B) The survival curve of xenograft mice revealed a short survival time for both UBDP1 overexpressing and UBD overexpressing groups. (C and D) Immunohistochemical staining of Ki67 (magnification, x40) indicated a significantly high proliferation index in UBDP1 or UBD overexpressing xenograft tumors. n=9. ***P<0.001. NC, negative control; OE, overexpression.

results confirmed that UBDP1 can competitively bind to miR-6072.

Discussion

Pseudogenes can competitively bind to miRNAs, thereby alleviating their inhibition of the expression of their parental genes and forming a regulatory network to promote tumor progression. In the present study, the upregulated pseudogene UBDP1 was identified in GBM, whose high expression was associated with poor prognosis. Further experiments demonstrated that UBDP1 increases the level of its oncogenic partner UBD by sponging miRNA-6072, thereby reinforcing the malignant phenotypes of glioma cells. The present findings revealed a tumor-promoting role of the UBDP1 and its functioning network with miR-6072 and UBD in glioma progression.

The UBD gene, located in the 6q21.3 region of the chromosome, is unique in encoding a ubiquitin-like protein that directly targets substrates for proteasomal degradation (26). UBD dysregulation has been reported in various cancers and can promote tumor progression through multiple pathways (27). Prior research has shown that UBD, via its ubiquitin-like domain, interacts with the spindle assembly checkpoint MAD2, thereby affecting mitotic regulation and contributing to tumor growth and malignancy (14). Furthermore, UBD forms a complex with translation elongation factor eEF1A1, competing with ubiquitin for binding, thus stabilizing eEF1A1 expression to foster tumor proliferation (28). High expression levels of MAD2 and eEF1A1 have been detected in gliomas, contributing to proliferation and survival of tumor cells (29-31). It is hypothesized that MAD2 and eEF1A1 may act as downstream to UBD in a protein-protein interaction manner during glioma progression.

Moreover, previous studies demonstrated that UBD influences gene expression at the transcription level. Findings indicated UBD suppresses the transcriptional activity of tumor suppressor p53, without significantly affecting its protein levels (32). The inactivation of p53, a phenomenon linked to commonly occurring cellular signaling pathways in glioma genesis, is exacerbated by UBD overactivation (33). UBD and p53 can form a regulatory loop, maintaining equilibrium between UBD and p53 levels which is crucial for

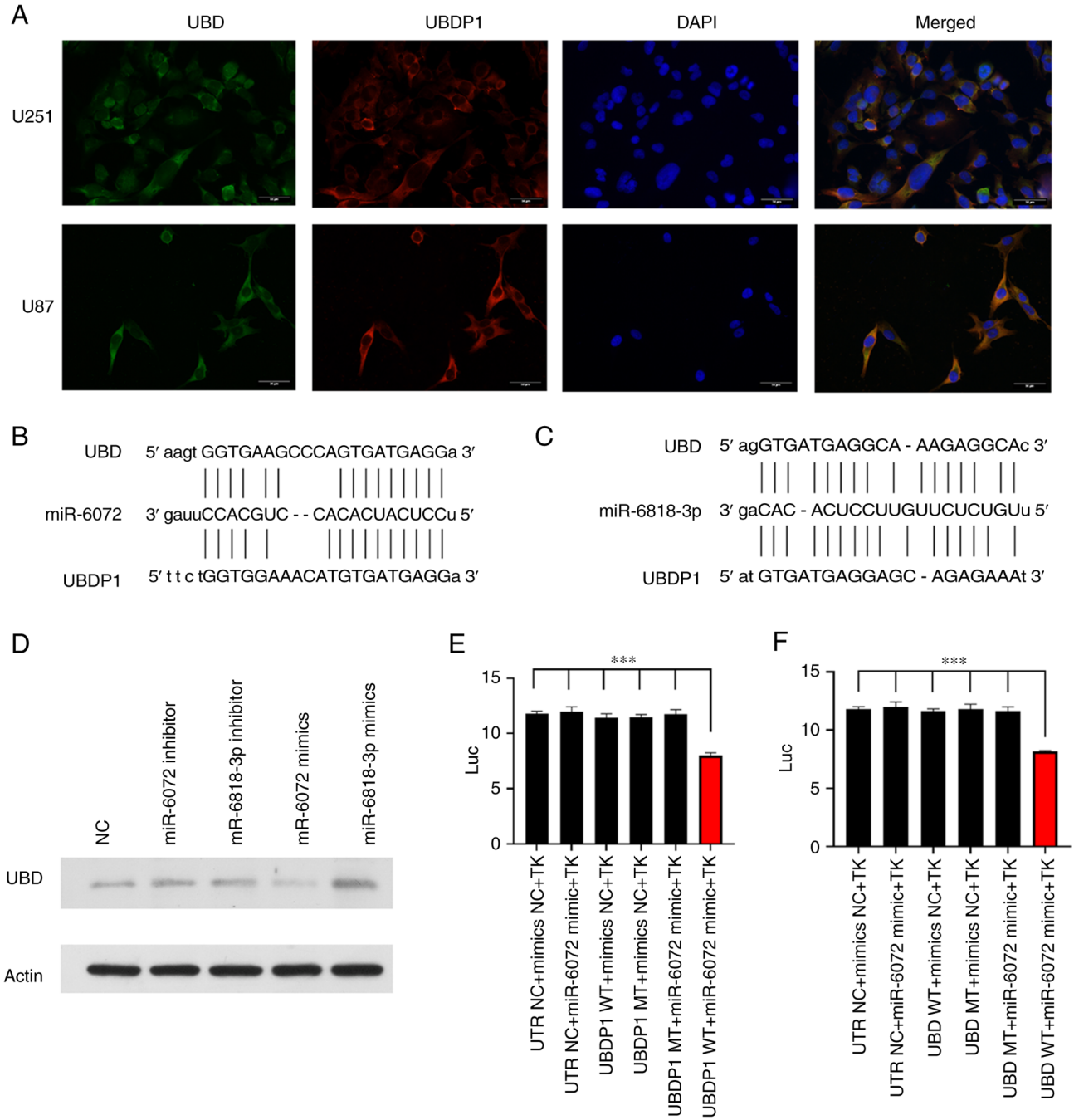

Figure 4. miR-6072 was identified to bind to both UBD and UBDP1. (A) Fluorescence in situ hybridization and immunofluorescence assay (magnification, x400) determined the subcellular localization of UBDP1 and UBD in the cytoplasm. (B and C) Sequencing analysis detected potential binding sites of miR-6072 and miR-6818-3p in UBD mRNA and UBDP1. (D) The expression of UBD protein in different conditions of miR-6072 or miR-6818-3p expression pattern was determined by western blotting. (E and F) WT or MT UBDP1 or UBD vectors were transfected into the 293T cell lines with or without synthetic miR-6072 mimics, and luciferase assays demonstrated significantly decreased luciferase activities in both WT UBDP1 and WT UBD groups with miR-6072 mimics. n=3. ***P<0.001. miR, microRNA; WT, wild-type; MT, mutant; NC, negative control.

the precise regulation of p53. When UBD is overexpressed, it suppresses the transcriptional activity of p53, which in turn, accelerates tumor development and progression (32). Interestingly, another study drew a different conclusion regarding UBD's overexpression leading to WISP1 protein/mRNA expression discrepancy (34). By stabilizing β-catenin, UBD overexpression increases WISP1 mRNA expression. While UBD stabilizes substrates simultaneously which increases WISP1 protein degradation, and thereby promoting the proliferation of hepatocellular carcinoma. However, coordinated expression of WISP1 protein and mRNA has been observed in glioma (35). WISP1, as a downstream effector of the Wnt/β-catenin pathway, is closely associated with glioma malignancy, promotes glioma cell proliferation, epithelial-mesenchymal transition, glioma stem cells maintenance and tumor-supportive macrophages in GBM (35-37). It is reasonable to assume that UBD upregulates WISP1 in glioma cells without suppressing its protein level, mediating oncogenic functions of Wnt/β-catenin signaling and contributing to glioma progression. The

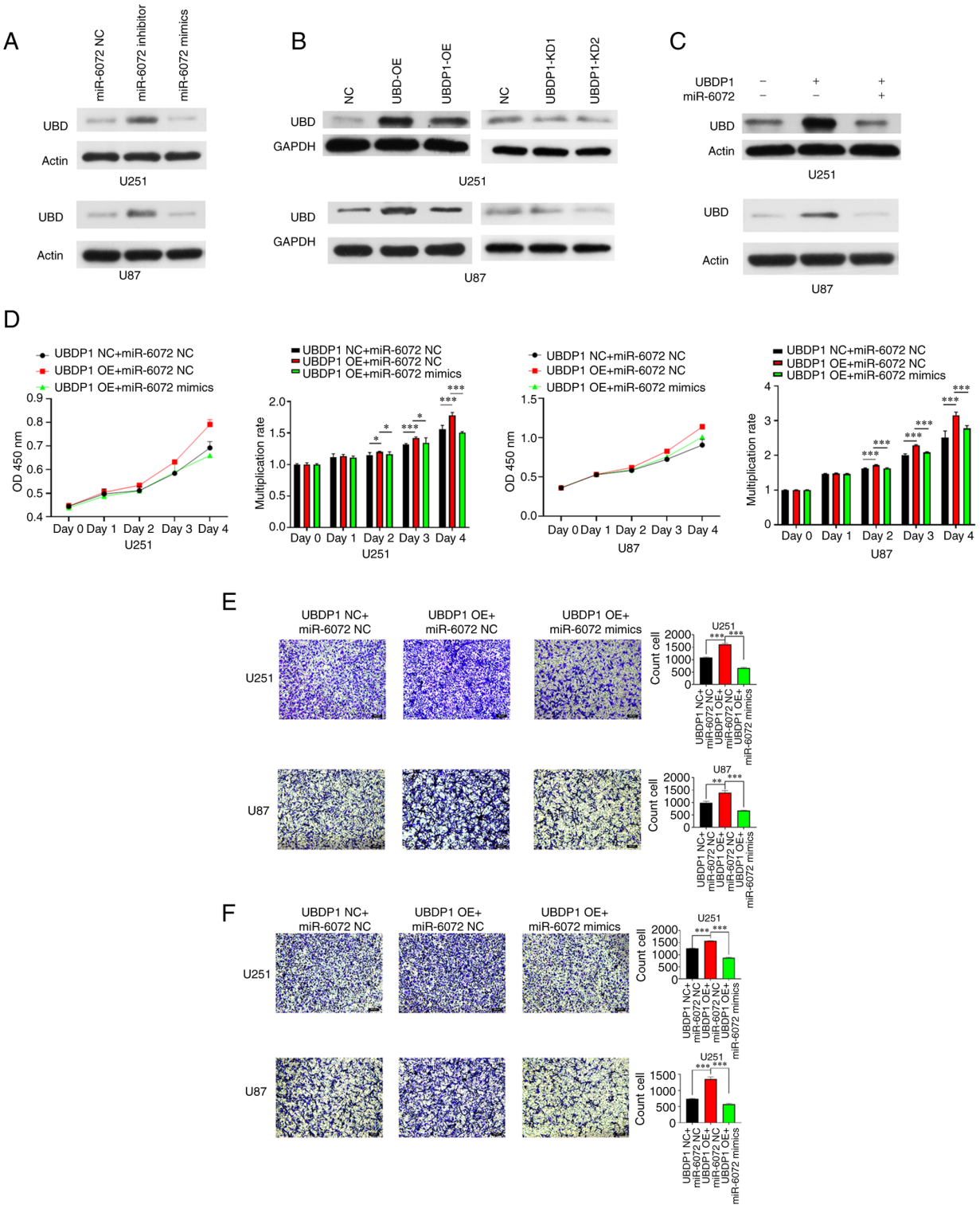

Figure 5. UBD and UBDP1 could competitively bind to miR-6072 in glioma. (A) Western blot analysis detected the expression of UBD protein in different conditions of miR-6072 expression pattern and found miR-6072 inhibitor significantly upregulating UBD expression. (B) The expression of UBD protein was increased in glioma cells with UBDP1 overexpression but was decreased in the condition of UBDP1 inhibition. (C) Elevated expression of UBD protein in glioma cells with UBDP1 could be restrained when cells were co-transfected with miR-6072 mimics. (D) Cell Counting Kit-8 assay demonstrated that enhanced proliferation ability of glioma cells induced by UBDP1 overexpression could be restored by miR-6072 mimics. (E and F) Transwell and Matrigel assays (magnification, x40) assessed the migration and invasion abilities of glioma cells in different conditions and revealed the inhibitory effects of miR-6072 mimics in glioma cells with UBDP1 overexpression. n=3. *P<0.05, **P<0.01 and ***P<0.001. miR, microRNA; KD, knockdown; NC, negative control; OE, overexpression.

mechanisms underlying the UBDP1/miRNA-6072/UBD regulatory network in glioma need to be further investigated for verification.

A xenograft GBM model was established in nude mice using the U87 cell line. The present *in vivo* studies revealed a significant correlation between elevated levels of UBDP1 and

UBD, decreased overall survival, and increased Ki-67 levels in xenograft mice compared with the control group. These findings strongly implicate the involvement of both UBDP1 and UBD in the oncogenic progression of GBM. However, previous research (38) has brought to light the origin of the U87 cell line. According to a previous study, the U87 cell line, while of central nervous system origin, is considered a *bona fide* human GBM cell line with an unknown patient origin, rather than the original GBM cell line established in 1968 at the University of Uppsala. Considering this revelation, it is imperative that future investigations replicate the current experiments using alternative stable GBM cell lines. This replication would serve to validate and reinforce the present findings, thereby bolstering reliability and generalizability.

The competing endogenous RNA hypothesis suggests that RNA molecules regulate gene expression by acting as miRNA sponges. This principle, widely demonstrated in cancer research, signifies a communication link between pseudogenes and their parental protein-coding genes. The present study indicated that miRNA-6072 can target both UBD and UBDP1, suggesting that UBDP1 partly regulates UBD expression by competitively binding with miRNA-6072, thereby influencing glioma progression. Additionally, emerging evidence shows that pseudogenes can affect their parental genes in various ways, either positively or negatively. For instance, pseudogenes can interact with proteins and localize to the promoters of their parental genes, which regulate target gene expression. Antisense RNA (asRNA) generated from pseudogenes can combine with sense-stranded mRNA from a homologous parent gene, affecting mRNA stability (39). A previous study demonstrated that PTENP1, a PTEN pseudogene, encodes an alpha asRNA isoform that localizes to the PTEN promoter, epigenetically modulating PTEN transcription by recruiting DNMT3a and EZH2. The beta asRNA isoform interacts with PTENP1, affecting its stability and miRNA sponge activity (40). In another study, pseudogene DUXAP10 was revealed to interact with PRC2 and LSD1, repressing LATS1 expression at the transcriptional level. It also binds with HuR, maintaining the stability of β-catenin mRNA and increasing its protein levels at the post-transcriptional level (41). As the understanding of pseudogenes has deepened, further mechanistic research is required to explore the potential effects of UBDP1 on UBD activity in glioma.

Numerous studies have elucidated the pivotal influence of tumor immune cell infiltration on the prognosis and therapeutic outcomes for cancer patients. As the role of the immune system in cancer development and progression becomes increasingly recognized, immunotherapy has witnessed rapid advancements. Effective immunotherapy against tumors necessitates sufficient immune cell infiltration within the tumor microenvironment. UBD exhibits heterogeneous expression across human tissues, high expression level was observed within immune system organs such as lymph nodes, thymus and spleen (42,43). The expression of UBD mRNA in organs involved in lymphocyte development, maturation and activity suggests a crucial role in the maturation process of lymphocytes (44,45). Under normal conditions, UBD is induced during the maturation process of dendritic cells triggered by toll-like receptor ligands, enhancing the potential for antigen presentation and stimulating T cells, thereby playing a key role in immune defense (46).

A recent study also indicated that pro-inflammatory cytokines such as interferon-γ, tumor necrosis factor-α and interleukin-6 can robustly stimulate FAT10 mRNA and protein levels across all tissues, potentially triggering widespread changes in cellular processes (47). Additionally, constitutive stimulation by these cytokines may promote DNA damage and aberrant tissue healing, creating a conducive environment for tumorigenesis.

It is crucial to acknowledge that the immune landscape of gliomas is not solely influenced by T cell populations. The absence of a broader immune cell profiling is a limitation of the present study. Other immune cells, including macrophages, natural killer cells and B cells, also contribute significantly to the immune dynamics within gliomas. Their roles, while not explored in the present study, could provide a more comprehensive understanding of the immune contexture and therapeutic responses. It is proposed by the authors that future research should expand on these findings to include a wide array of immune cells, which will help elucidate the complex interplay between UBD expression and the immune environment in gliomas.

In summary, the expression of UBD may affect lymphocytes at tumor sites, altering the efficacy of immune responses. The complex interplay between UBD expression, GBM progression and lymphocyte infiltration provides a promising avenue for future research, particularly in the evaluation of immunological markers. Prospective studies are encouraged to delve into the molecular mechanisms underlying UBD-mediated immune modulation, aiming to identify novel therapeutic targets. Advancing understanding of UBD's role in glioma immunology paves the way for the development of more precise and effective immunotherapeutic strategies, potentially transforming the clinical management of gliomas.

In conclusion, UBDP1 is upregulated in GBM and has the potential to serve as a prognostic biomarker for patients. Moreover, UBDP1 may enhance glioma progression by competitively binding with miRNA-6072 against its parental gene, UBD. These findings suggested that blocking the UBDP1/miRNA-6072/UBD network may represent a novel therapeutic approach for glioma.

Acknowledgements

Not applicable.

Funding

The present study was supported by the National Natural Science Foundation of China (grant nos. 81902538, 82272715, 82272904 and 81872072), the Shanghai Sailing Program (grant no. 19YF1448200) and the Shanghai Basic Research Program (grant no. 19JC1415000).

Availability of data and materials

The datasets used and/or analyzed during the current study are available from the corresponding author on reasonable request.

Authors' contributions

FH performed experimental operations and data analyses. FH, HW, ZG and TH wrote the manuscript. ZG and CC contributed significantly in data analyses and manuscript revision. JC and HW conceived and designed the study. TH, QH, ZG, YL, PM and XZ carried out the study and collected important background information. HW and JC confirm the authenticity of all the raw data. All authors read and approved the final manuscript.

Ethics approval and consent to participate

All methods in the present study were carried out in accordance with relevant guidelines and regulations and reported in accordance with ARRIVE guidelines for the reporting of animal experiments. Animal experiments were approved (approval no. CZEC2018-032) by the Animal Care and Experimental Committee of Naval Medical University (Shanghai, China). Human studies were approved (approval no. CZEC2018-032) by the Independent Ethics Committee of Naval Medical University (Shanghai, China). Written informed consents to participate in the present study were obtained from all patients or their legal guardians prior to study commencement.

Patient consent for publication

Not applicable.

Competing interests

The authors declare that they have no competing interests.

References

1. Taphoorn MJB, Dirven L, Kanner AA, Lavy-Shahaf G, Weinberg U, Taillibert S, Toms SA, Honnorat J, Chen TC, Sroubek J, *et al*: Influence of treatment with tumor-treating fields on health-related quality of life of patients with newly diagnosed glioblastoma: A secondary analysis of a randomized clinical trial. JAMA Oncol 4: 495-504, 2018.
2. Stupp R, Taillibert S, Kanner A, Read W, Steinberg D, Lhermitte B, Toms S, Idbaih A, Ahluwalia MS, Fink K, *et al*: Effect of tumor-treating fields plus maintenance temozolomide vs maintenance temozolomide alone on survival in patients with glioblastoma: A randomized clinical trial. JAMA 318: 2306-2316, 2017.
3. Pink RC and Carter DRF: Pseudogenes as regulators of biological function. Essays Biochem 54: 103-112, 2013.
4. Lou W, Ding B and Fu P: Pseudogene-derived lncRNAs and Their miRNA sponging mechanism in human cancer. Front Cell Dev Biol 8: 85, 2020.
5. Poliseno L, Salmena L, Zhang J, Carver B, Haveman WJ and Pandolfi PP: A coding-independent function of gene and pseudogene mRNAs regulates tumour biology. Nature 465: 1033-1038, 2010.
6. Chan JJ, Kwok ZH, Chew XH, Zhang B, Liu C, Soong TW, Yang H and Tay Y: A FTH1 gene:Pseudogene:microRNA network regulates tumorigenesis in prostate cancer. Nucleic Acids Res 46: 1998-2011, 2018.
7. Karreth FA, Reschke M, Ruocco A, Ng C, Chapuy B, Léopold V, Sjoberg M, Keane TM, Verma A, Ala U, *et al*: The BRAF pseudogene functions as a competitive endogenous RNA and induces lymphoma in vivo. Cell 161: 319-332, 2015.
8. Zhou D, Ren K, Wang M, Wang J, Li E, Hou C, Su Y, Jin Y, Zou Q, Zhou P and Liu X: Long non-coding RNA RACGAP1P promotes breast cancer invasion and metastasis via miR-345-5p/RACGAP1-mediated mitochondrial fission. Mol Oncol 15: 543-559, 2021.
9. Gao KM, Chen XC, Zhang JX, Wang Y, Yan W and You YP: A pseudogene-signature in glioma predicts survival. J Exp Clin Cancer Res 34: 23, 2015.
10. Wang Y, Liu X, Guan G, Xiao Z, Zhao W and Zhuang M: Identification of a five-pseudogene signature for predicting survival and its ceRNA network in glioma. Front Oncol 9: 1059, 2019.
11. Wang S, Qi Y, Gao X, Qiu W, Liu Q, Guo X, Qian M, Chen Z, Zhang Z, Wang H, *et al*: Hypoxia-induced lncRNA PDIA3P1 promotes mesenchymal transition via sponging of miR-124-3p in glioma. Cell Death Dis 11: 168, 2020.
12. Liao K, Qian Z, Zhang S, Chen B, Li Z, Huang R, Cheng L, Wang T, Yang R, Lan J, *et al*: The LGMN pseudogene promotes tumor progression by acting as a miR-495-3p sponge in glioblastoma. Cancer Lett 490: 111-123, 2020.
13. Du P, Liao Y, Zhao H, Zhang J, Muyiti, Keremu and Mu K: ANXA2P2/miR-9/LDHA axis regulates Warburg effect and affects glioblastoma proliferation and apoptosis. Cell Signal 74: 109718, 2020.
14. Theng SS, Wang W, Mah WC, Chan C, Zhuo J, Gao Y, Qin H, Lim L, Chong SS, Song J and Lee CG: Disruption of FAT10-MAD2 binding inhibits tumor progression. Proc Natl Acad Sci USA 111: E5282-E5291, 2014.
15. Yuan R, Wang K, Hu J, Yan C, Li M, Yu X, Liu X, Lei J, Guo W, Wu L, *et al*: Ubiquitin-like protein FAT10 promotes the invasion and metastasis of hepatocellular carcinoma by modifying β-catenin degradation. Cancer Res 74: 5287-5300, 2014.
16. Ma C, Zhang Z, Cui Y, Yuan H and Wang F: Silencing Fat10 inhibits metastasis of osteosarcoma. Int J Oncol 49: 666-674, 2016.
17. Zou Y, Ouyang Q, Wei W, Yang S, Zhang Y and Yang W: FAT10 promotes the invasion and migration of breast cancer cell through stabilization of ZEB2. Biochem Biophys Res Commun 506: 563-570, 2018.
18. Xue F, Zhu L, Meng QW, Wang L, Chen XS, Zhao YB, Xing Y, Wang XY and Cai L: FAT10 is associated with the malignancy and drug resistance of non-small-cell lung cancer. Onco Targets Ther 9: 4397-4409, 2016.
19. Yuan J, Tu Y, Mao X, He S, Wang L, Fu G, Zong J and Zhang Y: Increased expression of FAT10 is correlated with progression and prognosis of human glioma. Pathol Oncol Res 18: 833-839, 2012.
20. Dai B, Zhang Y, Zhang P, Pan C, Xu C, Wan W, Wu Z, Zhang J and Zhang L: Upregulation of p-Smad2 contributes to FAT10-induced oncogenic activities in glioma. Tumour Biol 37: 8621-8631, 2016.
21. Yan Y, Zhang L, Jiang Y, Xu T, Mei Q, Wang H, Qin R, Zou Y, Hu G, Chen J and Lu Y: LncRNA and mRNA interaction study based on transcriptome profiles reveals potential core genes in the pathogenesis of human glioblastoma multiforme. J Cancer Res Clin Oncol 141: 827-838, 2015.
22. Livak KJ and Schmittgen TD: Analysis of relative gene expression data using real-time quantitative PCR and the 2(-Delta Delta C(T)) method. Methods 25: 402-408, 2001.
23. Zhou J, Wang H, Hong F, Hu S, Su X, Chen J and Chu J: CircularRNA circPARP4 promotes glioblastoma progression through sponging miR-125a-5p and regulating FUT4. Am J Cancer Res 11: 138-156, 2021.
24. He H, Wang Y, Ye P, Yi D, Cheng Y, Tang H, Zhu Z, Wang X and Jin S: Long noncoding RNA ZFPM2-AS1 acts as a miRNA sponge and promotes cell invasion through regulation of miR-139/GDF10 in hepatocellular carcinoma. J Exp Clin Cancer Res 39: 159, 2020.
25. Cui Y, Yi L, Zhao JZ and Jiang YG: Long noncoding RNA HOXA11-AS functions as miRNA sponge to promote the glioma tumorigenesis through targeting miR-140-5p. DNA Cell Biol 36: 822-828, 2017.
26. Zhang JY, Wang M, Tian L, Genovese G, Yan P, Wilson JG, Thadhani R, Mottl AK, Appel GB, Bick AG, *et al*: UBD modifies APOL1-induced kidney disease risk. Proc Natl Acad Sci USA 115: 3446-3451, 2018.
27. Aichem A and Groettrup M: The ubiquitin-like modifier FAT10 in cancer development. Int J Biochem Cell Biol 79: 451-461, 2016.
28. Liu X, Chen L, Ge J, Yan C, Huang Z, Hu J, Wen C, Li M, Huang D, Qiu Y, *et al*: The ubiquitin-like protein FAT10 stabilizes eEF1A1 expression to promote tumor proliferation in a complex manner. Cancer Res 76: 4897-4907, 2016.
29. Wu D, Wang L, Yang Y, Huang J, Hu Y, Shu Y, Zhang J and Zheng J: MAD2-p31^{comet} axis deficiency reduces cell proliferation, migration and sensitivity of microtubule-interfering agents in glioma. Biochem Biophys Res Commun 498: 157-163, 2018.

30. Scrideli CA, Carlotti CG Jr, Okamoto OK, Andrade VS, Cortez MAA, Motta FJN, Lucio-Eterovic AK, Neder L, Rosemberg S, Oba-Shinjo SM, *et al*: Gene expression profile analysis of primary glioblastomas and non-neoplastic brain tissue: Identification of potential target genes by oligonucleotide microarray and real-time quantitative PCR. J Neurooncol 88: 281-291, 2008.
31. Biterge-Sut B: Alterations in eukaryotic elongation factor complex proteins (EEF1s) in cancer and their implications in epigenetic regulation. Life Sci 238: 116977, 2019.
32. Choi Y, Kim JK and Yoo JY: NFκB and STAT3 synergistically activate the expression of FAT10, a gene counteracting the tumor suppressor p53. Mol Oncol 8: 642-655, 2014.
33. Wang H, Xu T, Jiang Y, Xu H, Yan Y, Fu D and Chen J: The challenges and the promise of molecular targeted therapy in malignant gliomas. Neoplasia 17: 239-255, 2015.
34. Yan J, Lei J, Chen L, Deng H, Dong D, Jin T, Liu X, Yuan R, Qiu Y, Ge J, *et al*: Human leukocyte antigen F locus adjacent transcript 10 overexpression disturbs WISP1 protein and mRNA expression to promote hepatocellular carcinoma progression. Hepatology 68: 2268-2284, 2018.
35. Jing D, Zhang Q, Yu H, Zhao Y and Shen L: Identification of WISP1 as a novel oncogene in glioblastoma. Int J Oncol 51: 1261-1270, 2017.
36. Tao W, Chu C, Zhou W, Huang Z, Zhai K, Fang X, Huang Q, Zhang A, Wang X, Yu X, *et al*: Dual role of WISP1 in maintaining glioma stem cells and tumor-supportive macrophages in glioblastoma. Nat Commun 11: 3015, 2020.
37. He L, Zhou H, Zeng Z, Yao H, Jiang W and Qu H: Wnt/β-catenin signaling cascade: A promising target for glioma therapy. J Cell Physiol 234: 2217-2228, 2019.
38. Allen M, Bjerke M, Edlund H, Nelander S and Westermark B: Origin of the U87MG glioma cell line: Good news and bad news. Sci Transl Med 8: 354re3, 2016.
39. Chen X, Wan L, Wang W, Xi WJ, Yang AG and Wang T: Re-recognition of pseudogenes: From molecular to clinical applications. Theranostics 10: 1479-1499, 2020.
40. Johnsson P, Ackley A, Vidarsdottir L, Lui WO, Corcoran M, Grandér D and Morris KV: A pseudogene long-noncoding-RNA network regulates PTEN transcription and translation in human cells. Nat Struct Mol Biol 20: 440-446, 2013.
41. Xu Y, Yu X, Wei C, Nie F, Huang M and Sun M: Over-expression of oncigenic pesudogene DUXAP10 promotes cell proliferation and invasion by regulating LATS1 and β-catenin in gastric cancer. J Exp Clin Cancer Res 37: 13, 2018.
42. Lee CGL, Ren J, Cheong ISY, Ban KHK, Ooi LLPJ, Yong Tan S, Kan A, Nuchprayoon I, Jin R, Lee KH, *et al*: Expression of the FAT10 gene is highly upregulated in hepatocellular carcinoma and other gastrointestinal and gynecological cancers. Oncogene 22: 2592-2603, 2003.
43. Lukasiak S, Schiller C, Oehlschlaeger P, Schmidtke G, Krause P, Legler DF, Autschbach F, Schirmacher P, Breuhahn K and Groettrup M: Proinflammatory cytokines cause FAT10 upregulation in cancers of liver and colon. Oncogene 27: 6068-6074, 2008.
44. Buerger S, Herrmann VL, Mundt S, Trautwein N, Groettrup M and Basler M: The ubiquitin-like modifier FAT10 is selectively expressed in medullary thymic epithelial cells and modifies T cell selection. J Immunol 195: 4106-4116, 2015.
45. Canaan A, Yu X, Booth CJ, Lian J, Lazar I, Gamfi SL, Castille K, Kohya N, Nakayama Y, Liu YC, *et al*: FAT10/diubiquitin-like protein-deficient mice exhibit minimal phenotypic differences. Mol Cell Biol 26: 5180-1589, 2006.
46. Basler M, Buerger S and Groettrup M: The ubiquitin-like modifier FAT10 in antigen processing and antimicrobial defense. Mol Immunol 68: 129-132, 2015.
47. Kandel-Kfir M, Garcia-Milan R, Gueta I, Lubitz I, Ben-Zvi I, Shaish A, Shir L, Harats D, Mahajan M, Canaan A andf Kamari Y: IFNγ potentiates TNFα/TNFR1 signaling to induce FAT10 expression in macrophages. Mol Immunol 117: 101-109, 2020.